

*V.G. Labunets<sup>1</sup>, V.P. Chasovskikh<sup>1</sup>, E. Ostheimer<sup>2</sup>*

<sup>1</sup>Ural State Forest Engineering University, Yekaterinburg

<sup>2</sup>Capricat LLC 1340 S. Ocean Blvd., Suite 209 Pompano Beach, 33062 Florida, USA

## ALGEBRA AND GEOMETRY OF MULTICHANNEL IMAGES. PART 2. ORTHO-UNITARY TRANSFORMS, WAVELETS AND SPLINES

### Introduction

We present a new theoretical framework for multidimensional image processing using hypercomplex commutative algebras that codes color, multicolor and hypercolor. In this paper a family of discrete color-valued and multicolor-valued 2-D Fourier-like, wavelet-like transforms and splines has been presented that can be used in color, multicolor, and hyperspectral image processing. In our approach, each multichannel pixel is considered not as an  $K$ -D vector, but as an  $K$ -D hypercomplex number, where  $K$  is the number of different optical channels. Orthounitary transforms and splines are Centaurus (specific combination) of orthogonal and unitary transforms. It is known that Centaurus is a combination of half-man and half-horse. By this reason we can call an ortho-unitary (color) transform as a Centaurus of orthogonal and unitary transforms. We present several examples of possible Centauruses: Fourier+Walsh, Complex Walsh+Ordinary Walsh and so on. We collect basis functions of these transforms in the form of iconostas (in a Russian orthodox church, the "Iconostas" is literally the "Stand of Icons" that rise up at the front of the Sanctuary). These transforms are applicable to multichannel images with several components and are different from the classical Fourier transform in that they mix the channel components of the image. They can be used for multichannel images compression, interpolation and edge detection from the point of view of hypercomplex commutative algebras.

### Orthounitary transforms for color images processing

Classical Fourier analysis based on the orthogonal and unitary transforms plays an important role in digital image processing. Transforms, notable the classical Discrete Fourier Transform (DFT), are extensively used in digital image processing (filtering, power spectrum estimation, and so on). A natural question that arises in our approach is the definition of color and multicolor transforms that can be used efficiently in color and multicolor image processing. We propose a wide library of so-called orthounitary (color-valued or multicolor-valued) Fourier transforms for using in image compression, processing, and pattern recognition applications.

2-D discrete color ( $N \times N$ )-image  $\mathbf{f} := [\mathbf{f}(i, j)]_{i,j=1}^N$  can be defined as a 2-D ( $N \times N$ )-array in the (R,G,B) or (LC) formats (Greaves, 1847; Labunets et al., 2016):

$$\begin{aligned} \mathbf{f}(i, j) &= f_R(i, j)\mathbf{1} + f_G(i, j)\varepsilon + f_B(i, j)\varepsilon^2 : \mathbf{Z}_N^2 \rightarrow \text{Alg}_3^{\text{vis}}(\mathbf{R}|\mathbf{1}, \varepsilon, \varepsilon^2), \\ \mathbf{f}(i, j) &= f_{lu}(i, j)\mathbf{e}_{lu} + f_{ch}(i, j)\mathbf{E}_{ch} = (f_{lu}(i, j), f_{ch}(i, j)) : \mathbf{Z}_N^2 \rightarrow \mathbf{R} \oplus \mathbf{C}. \end{aligned} \quad (2)$$

where  $\mathbf{Z}_N^2$  is 2-D ( $N \times N$ )-array. Here, every color pixel  $\mathbf{f}(i, j)$  at position  $(i, j)$  is a triplet number in (R,G,B)- or in LC-formats, respectively and

$$\|\mathbf{f}(i, j)\|_2^2 =$$

$$= \sum \sum [f_r^2(i, j) + f_g^2(i, j) + f_b^2(i, j) - f_r(i, j)f_g(i, j) - f_r(i, j)f_b(i, j) - f_g(i, j)f_b(i, j)]$$

is norm of the image  $\mathbf{f}(i, j)$ .

All images  $\mathbf{f} := [\mathbf{f}(i, j)]_{i,j=1}^N$  form  $N^2$ -dimension space over the triplet algebra:  $(\text{Alg}_3^{\text{vis}})^{N^2}$ . We say the operator

$$L_{2D} : (\text{Alg}_3^{\text{vis}})^{N^2} \rightarrow (\text{Alg}_3^{\text{vis}})^{N^2} \text{ (or } L_{2D}[\mathbf{f}_{col}] = \mathbf{F}_{col})$$

is *ortho-unitary* if it conserves the norm of color images.

**Remark 1.** It should be noted that orthogonal transforms keep the norm of real-valued (gray-level) images, unitary transforms keep the norm of complex-valued (bichromatic) images. For this reason, ortho-unitary transforms are a generalization of orthogonal and unitary transforms for color images.

LC format ortho-unitary transforms can be constructed with help an orthogonal  $\mathbf{O}_{2D}$  and unitary  $\mathbf{U}_{2D}$  transforms  $L_{2D} = \mathbf{O}_{2D}\mathbf{e}_{lu} + \mathbf{U}_{2D}\mathbf{E}_{ch} = (\mathbf{O}_{2D}, \mathbf{U}_{2D})$ . The simplest form of ortho-unitary transform for image processing is a separable 2-D transform formed from two 1-D transforms by tensor product  $L_{2D} = (\mathbf{O}_1 \otimes \mathbf{O}_2)\mathbf{e}_{lu} + (\mathbf{U}_1 \otimes \mathbf{U}_2)\mathbf{E}_{ch}$ , where  $\otimes$  is the symbol of tensor product.

Application of separable transforms reduces the problem of designing efficient ortho-unitary 2-D transforms to a one-dimensional problem. It is possible to use one pair of orthogonal and unitary transforms, when  $\mathbf{O}_1 = \mathbf{O}_2 = \mathbf{O}$  and  $\mathbf{U}_1 = \mathbf{U}_2 = \mathbf{U}$ . Every pair  $(\mathbf{O}, \mathbf{U})$  of an orthogonal  $\mathbf{O}$  and an unitary  $\mathbf{U}$  transforms generates ortho-unitary (triplet-valued) 1D  $L_{1D} = \mathbf{O}\mathbf{e}_{lu} + \mathbf{U}\mathbf{E}_{ch}$  and 2-D ortho-unitary transforms:  $L_{2D} = (\mathbf{O} \otimes \mathbf{O})\mathbf{e}_{lu} + (\mathbf{U} \otimes \mathbf{U})\mathbf{E}_{ch}$ . They are *Centaurus* of orthogonal and unitary transforms.

**Remark 2.** It is known that *Centaurus* is a combination of half-men and half-horse. By this reason we can called an ortho-unitary (color) transform as a *Centaurus* of orthogonal and unitary transforms (Labunets-Rundblad et al., 2003a,b).

Some examples of possible Centuaruses (ortho-unitary transforms) are shown in the Table 1, where **W**, **Hd**, **Ht**, **Hr**, **Wv** are Walsh, Hadamard, Hartley, Haar, and Wavelet orthogonal transforms, respectively, and **F**, **W**, **Hd**, **Wv** are Fourier, complex Walsh, complex Hadamard and complex wavelet transforms, respectively.

**Table 1:** Centauruses of orthogonal and unitary transforms

	<b>F</b>	<b>W</b>	<b>Hd</b>	<b>Wv</b>
<b>W</b>	$\mathbf{W} \cdot \mathbf{e}_{lu} + \mathbf{F} \cdot \mathbf{E}_{ch}$	$\mathbf{W} \cdot \mathbf{e}_{lu} + \mathbf{W} \cdot \mathbf{E}_{ch}$	$\mathbf{W} \cdot \mathbf{e}_{lu} + \mathbf{Hd} \cdot \mathbf{E}_{ch}$	$\mathbf{W} \cdot \mathbf{e}_{lu} + \mathbf{Wv} \cdot \mathbf{E}_{ch}$
<b>Hd</b>	$\mathbf{Hd} \cdot \mathbf{e}_{lu} + \mathbf{F} \cdot \mathbf{E}_{ch}$	$\mathbf{Hd} \cdot \mathbf{e}_{lu} + \mathbf{W} \cdot \mathbf{E}_{ch}$	$\mathbf{Hd} \cdot \mathbf{e}_{lu} + \mathbf{Hd} \cdot \mathbf{E}_{ch}$	$\mathbf{Hd} \cdot \mathbf{e}_{lu} + \mathbf{Wv} \cdot \mathbf{E}_{ch}$
<b>Ht</b>	$\mathbf{Ht} \cdot \mathbf{e}_{lu} + \mathbf{F} \cdot \mathbf{E}_{ch}$	$\mathbf{Ht} \cdot \mathbf{e}_{lu} + \mathbf{W} \cdot \mathbf{E}_{ch}$	$\mathbf{Ht} \cdot \mathbf{e}_{lu} + \mathbf{Hd} \cdot \mathbf{E}_{ch}$	$\mathbf{Ht} \cdot \mathbf{e}_{lu} + \mathbf{Wv} \cdot \mathbf{E}_{ch}$
<b>Hr</b>	$\mathbf{Hr} \cdot \mathbf{e}_{lu} + \mathbf{F} \cdot \mathbf{E}_{ch}$	$\mathbf{Hr} \cdot \mathbf{e}_{lu} + \mathbf{W} \cdot \mathbf{E}_{ch}$	$\mathbf{Hr} \cdot \mathbf{e}_{lu} + \mathbf{Hd} \cdot \mathbf{E}_{ch}$	$\mathbf{Hr} \cdot \mathbf{e}_{lu} + \mathbf{Wv} \cdot \mathbf{E}_{ch}$
<b>Wv</b>	$\mathbf{Wv} \cdot \mathbf{e}_{lu} + \mathbf{F} \cdot \mathbf{E}_{ch}$	$\mathbf{Wv} \cdot \mathbf{e}_{lu} + \mathbf{W} \cdot \mathbf{E}_{ch}$	$\mathbf{Wv} \cdot \mathbf{e}_{lu} + \mathbf{Hr} \cdot \mathbf{E}_{ch}$	$\mathbf{Wv} \cdot \mathbf{e}_{lu} + \mathbf{Wv} \cdot \mathbf{E}_{ch}$

If  $\mathbf{O} = [\varphi_k(n)]_{k,n=0}^{N-1}$  and  $\mathbf{U} = [\psi_k(n)]_{k,n=0}^{N-1}$  are an orthogonal and unitary transforms with real-valued and complex-valued basis functions  $\{\varphi_k(n)\}_{k,n=0}^{N-1}$  and  $\{\psi_k(n)\}_{k,n=0}^{N-1}$ , respectively, then

$$\begin{aligned} & (\mathbf{O} \otimes \mathbf{O})\mathbf{e}_{lu} + (\mathbf{U} \otimes \mathbf{U})\mathbf{E}_{ch} = \\ & = ([\varphi_{k_1}(n_1)] \otimes [\varphi_{k_2}(n_2)])\mathbf{e}_{lu} + [\psi_{k_1}(n_1)] \otimes [\psi_{k_2}(n_2)]\mathbf{E}_{ch} = \\ & = [\varphi_{k_1}(n_1)\varphi_{k_2}(n_2)]\mathbf{e}_{lu} + [\psi_{k_1}(n_1)\psi_{k_2}(n_2)]\mathbf{E}_{ch}, \end{aligned} \quad (3)$$

is ortho-unitary transform, where  $\{\varphi_{k_1}(n_1)\varphi_{k_2}(n_2)\}_{k_1,k_2=0, n_1,n_2=0}^{N-1, N-1}$  and  $\{\psi_{k_1}(n_1)\psi_{k_2}(n_2)\}_{k_1,k_2=0, n_1,n_2=0}^{N-1, N-1}$  are  $N^2$  orthogonal and unitary basis ( $(N \times N)$ -pictures). We are going to collect them in the form of *iconostas* (in a Russian orthodox church, the "Iconostas" is literally the "Stand of Icons" that rise up at the front of the Sanctuary). For example, Iconostasis of Walsh, Cosine and Haar transforms shown in Fig. 1. Some examples of Iconostasis of *Centaurus* transforms shown in Fig. 2.

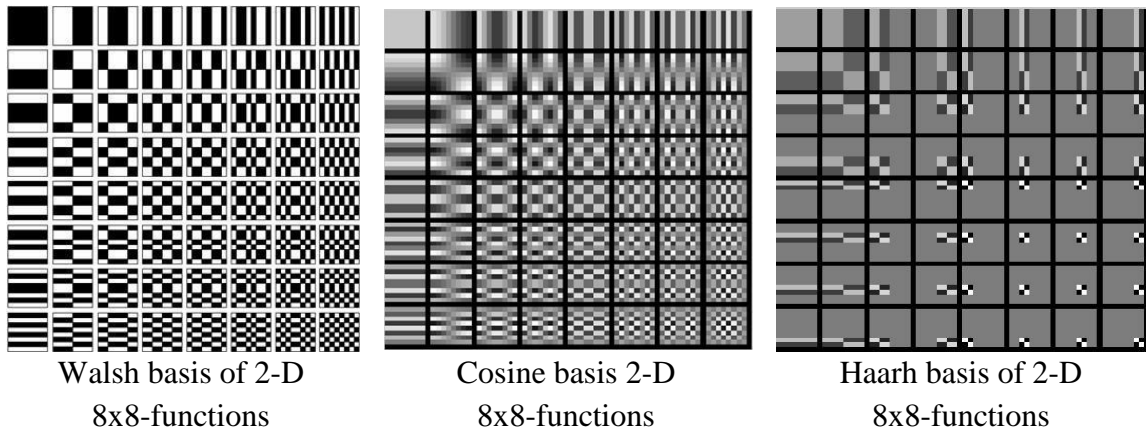


**Figure 1:** Iconostasis of 2D Basis Functions of Orthogonal transforms

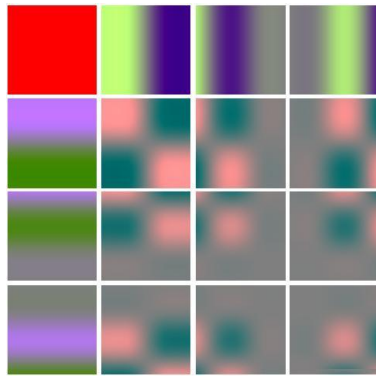
### Ortho-unitary wavelets

Let a real-valued mother wavelet  $\psi^R(x)$  and its scaled and shifted versions

$$\psi_{s,\tau}^R(x) = \frac{1}{\sqrt{|s|}} \psi^R\left(\frac{x-\tau}{s}\right), \quad s, \tau \in \mathbf{R}, \quad s \neq 0 \quad (4)$$

form an orthogonal basis of the space  $L_2(\mathbf{R})$ . We define the chromatic wavelet as the following (Labunets-Rundblad et al., 2001; Labunets et al., 2002):

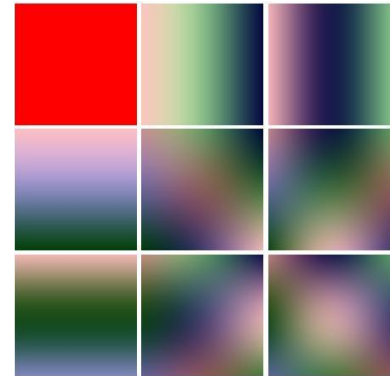
$$\begin{aligned} \psi_{s,\tau}^{Ch}(x) &= \psi_{s,\tau}^{\text{Re}}(x) + j\mathbf{H} \left\{ \psi_{s,\tau}^{\text{Re}}(x) \right\} = \psi_{s,\tau}^{\text{Re}}(x) + i\psi_{s,\tau}^{\text{Im}}(x) = \\ &= \frac{1}{\sqrt{|s|}} \psi^{\text{Re}}\left(\frac{x-\tau}{s}\right) + i \frac{1}{\sqrt{|s|}} \psi^{\text{Im}}\left(\frac{x-\tau}{s}\right), \end{aligned} \quad (5)$$



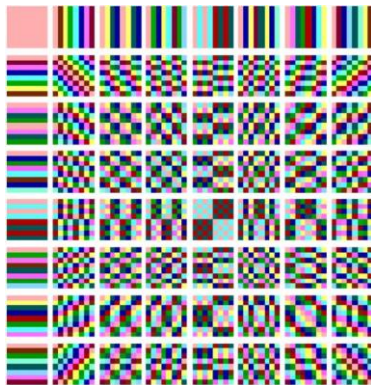
Color Walsh+Complex  
Walsh basis of 2-D  
4x4-functions



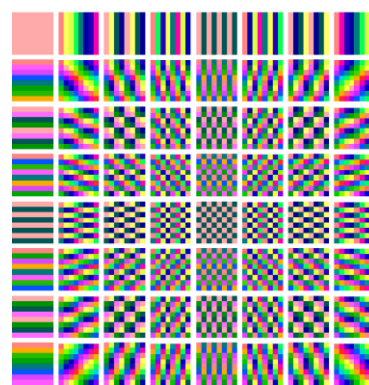
Color Walsh+Fourier  
basis of 2-D  
4x4-functions



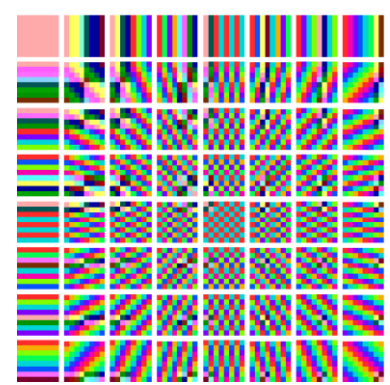
Color Hartley+Fourier  
basis of 2-D  
3x3-functions



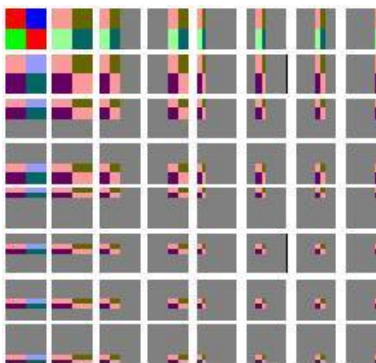
Color Walsh+Fourier  
basis of 2-D  
8x8-functions



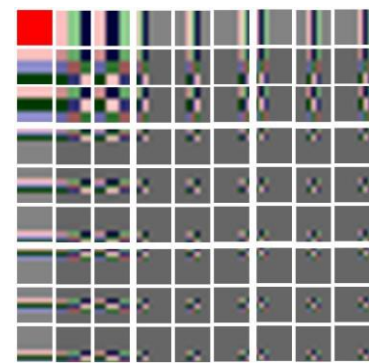
Color Hartley+Fourier  
basis of 2-D  
8x8-functions



Color Haar+Fourier  
basis of 2-D  
8x8-functions



Color ComplWalsh+Walsh  
basis of 2-D  
8x8-functions



Color Goley+Fourier  
basis of 2-D  
9x9-functions



Color Haar+Fresnel  
basis of 2-D  
9x9-functions

where  $\psi_{s,\tau}^{\text{Im}}(x) := \mathcal{H} \left\{ \psi_{s,\tau}^{\text{Re}}(x) \right\}$  is the Hilbert transform of the real-valued mother wavelet (4).

Now we construct triplet-valued (color) wavelet basis by

$$\begin{aligned} \psi_{s,\tau}^{\text{Col}}(x) &= \varphi_{s,\tau}^{\text{lu}}(x) \cdot \mathbf{e}_{\text{lu}} + \psi_{s,\tau}^{\text{Ch}}(x) \cdot \mathbf{E}_{\text{Ch}} = \\ &= \varphi_{s,\tau}^{\text{lu}}(x) \cdot \mathbf{e}_{\text{lu}} + \left[ \psi_{s,\tau}^{\text{Re}}(x) + j\mathcal{H} \left\{ \psi_{s,\tau}^{\text{Re}}(x) \right\} \right] \cdot \mathbf{E}_{\text{Ch}}. \end{aligned} \quad (6)$$

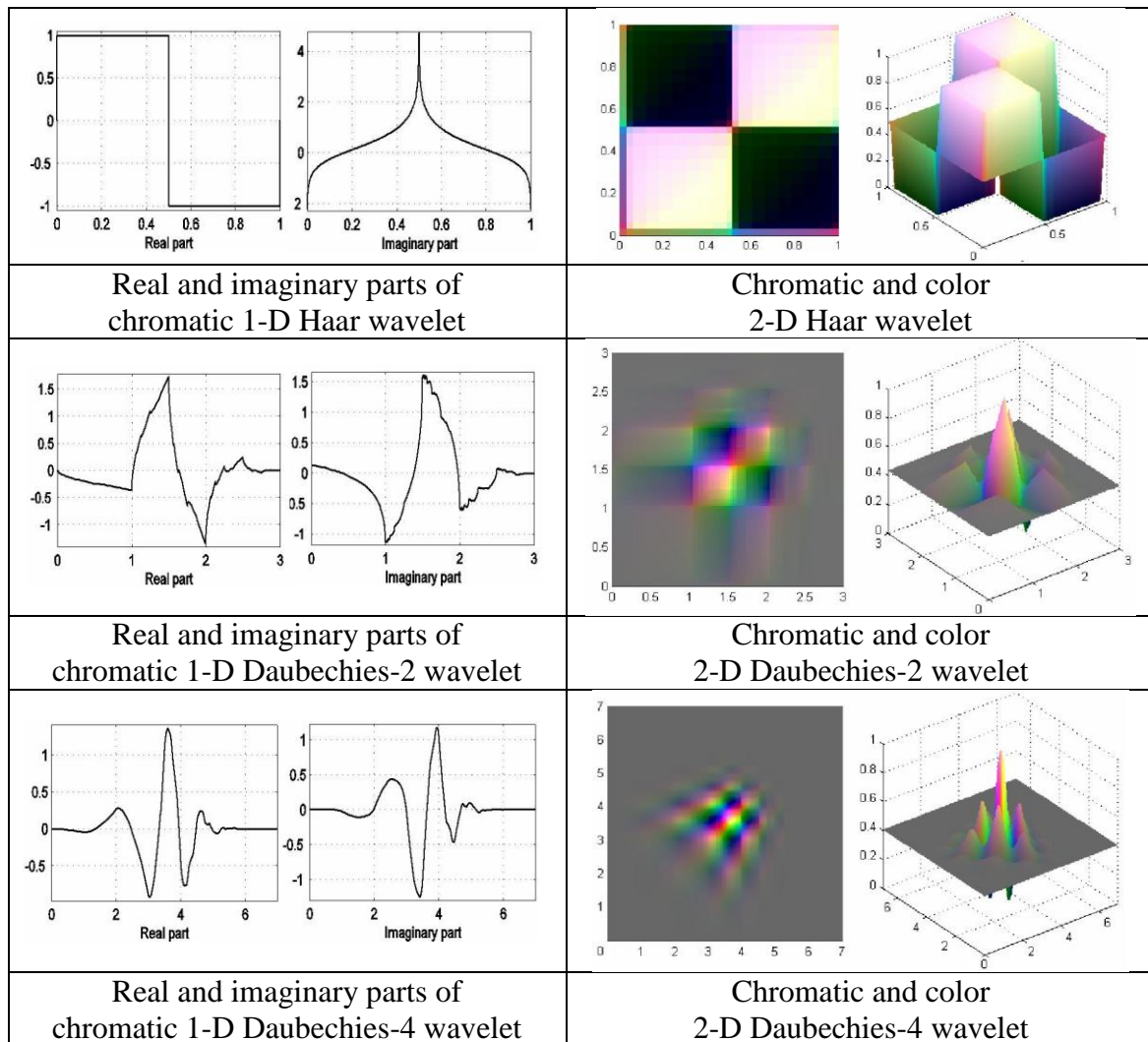
where  $\varphi_{s,\tau}^{lu}(x)$  is a real-valued wavelet basis for luminance terms and  $\psi_{s,\tau}^{Ch}(x)$  is a complex-valued wavelet basis for chromatic term. We can take  $\varphi_{s,\tau}^{lu}(x) \equiv \psi_{s,\tau}^{Re}(x)$ . In this case we obtain a color wavelet generated by a single real-valued wavelet  $\psi_{s,\tau}^{Re}(x)$ :

$$\begin{aligned}\psi_{s,\tau}^{Col}(x) &= \psi_{s,\tau}^{Re}(x) \cdot \mathbf{e}_{lu} + \left[ \psi_{s,\tau}^{Re}(x) + jH\{\psi_{s,\tau}^{Re}(x)\} \right] \cdot \mathbf{E}_{Ch} = \\ &= \psi_{s,\tau}^{Re}(x) \cdot [\mathbf{e}_{lu} + \mathbf{E}_{Ch}] + jH\{\psi_{s,\tau}^{Re}(x)\} \cdot \mathbf{E}_{Ch}.\end{aligned}\quad (7)$$

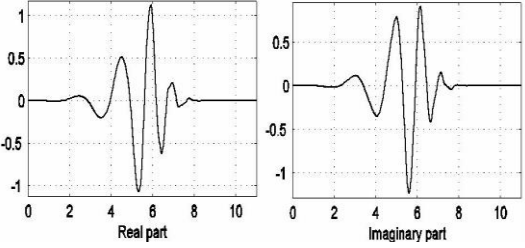
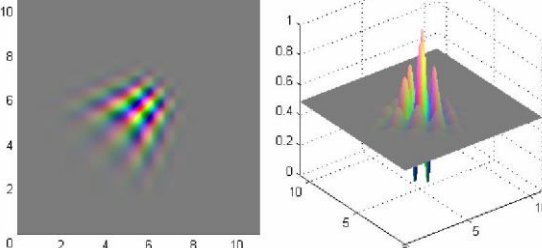
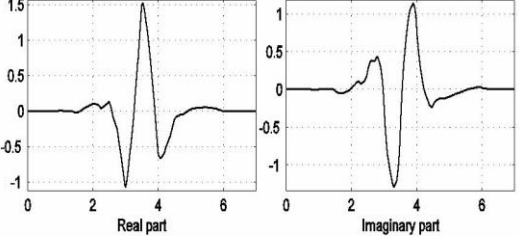
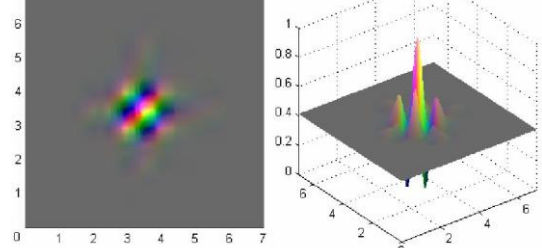
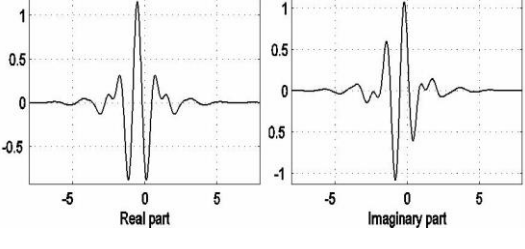
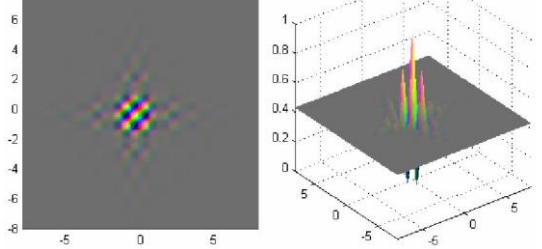
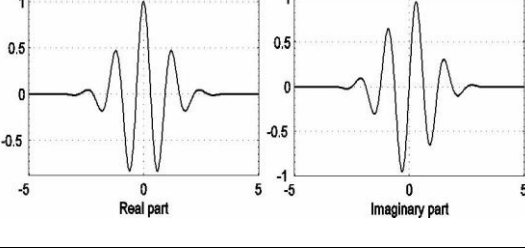
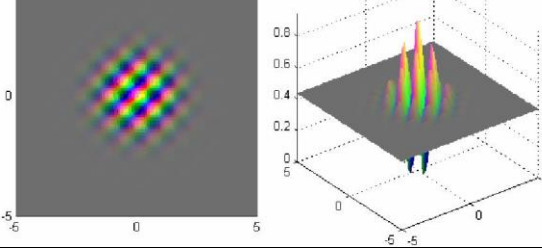
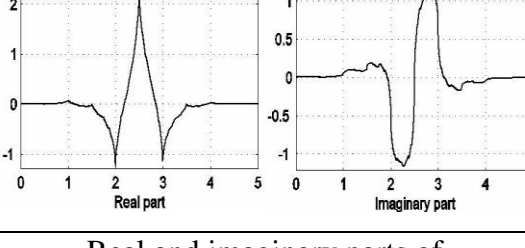
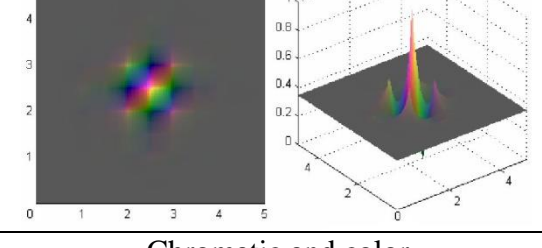
We define 2-D direct triplet-valued (color) *continuous orthounitary wavelet transform* (COUT) by

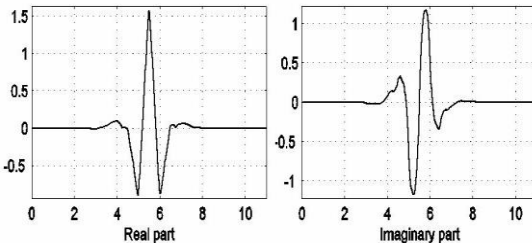
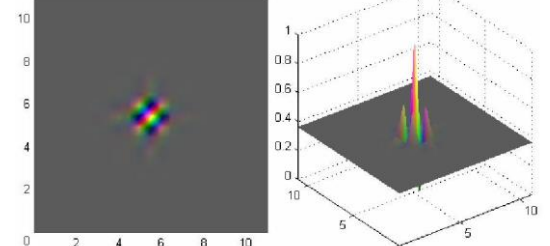
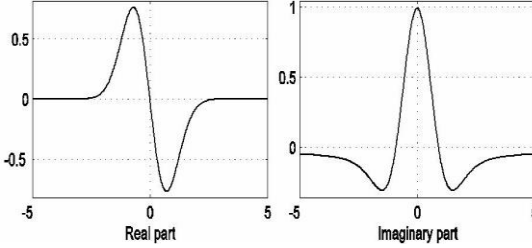
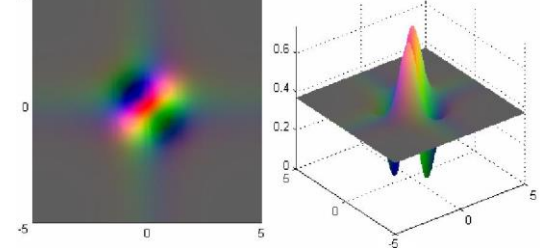
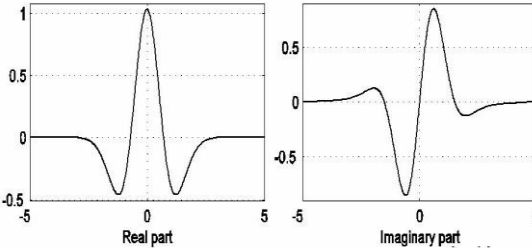
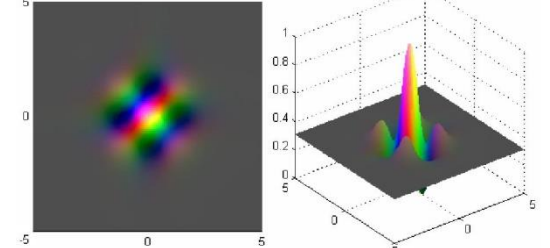
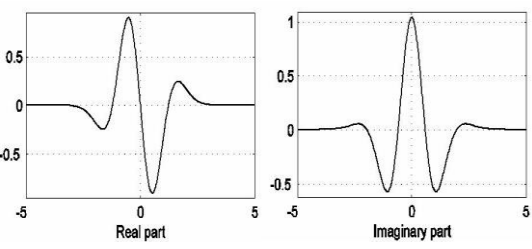
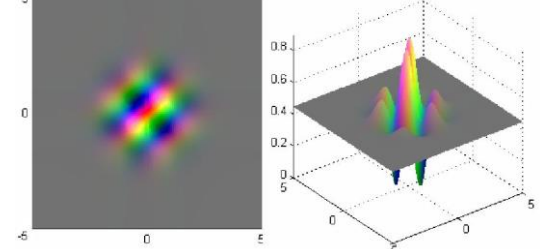
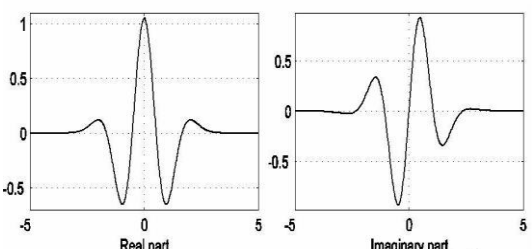
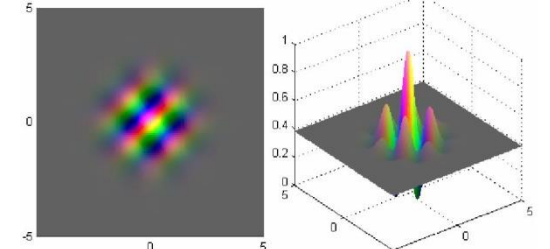
$$F_{COUT}^{col}(s_1, \tau_1, s_2, \tau_2) = \frac{1}{\sqrt{|s_1||s_2|}} \int_{-\infty}^{+\infty} \int_{-\infty}^{+\infty} \mathbf{f}_{col}(x, y) \psi_{s,\tau}^{Col}(x) \psi_{s,\tau}^{Col}(y) dx dy. \quad (8)$$

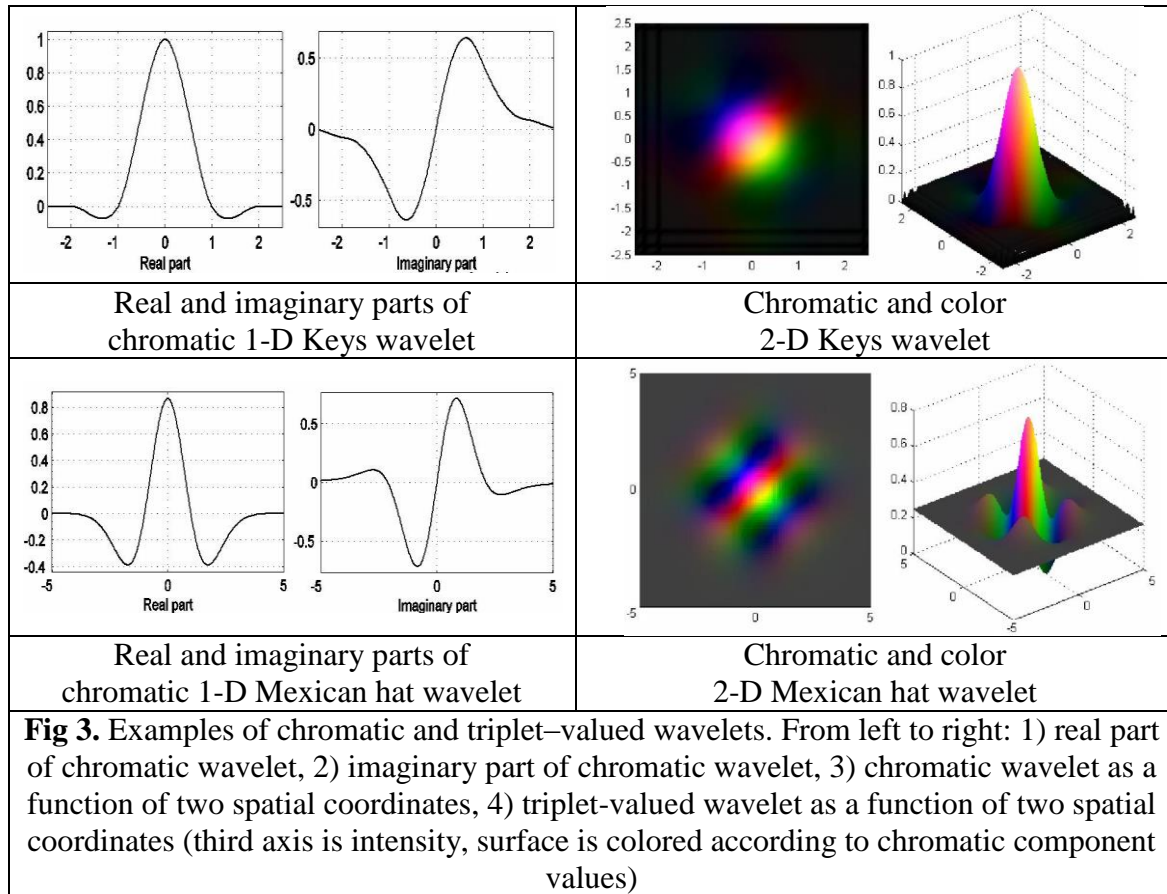
Examples of chromatic and triplet-valued wavelets are shown in Fig. 3. They are *Centaurus* of orthogonal and unitary wavelets.





	
<p>Real and imaginary parts of Chromatic 1-D Daubechies-6 wavelet</p>	<p>Chromatic and color 2-D Daubechies-6 wavelet</p>
	
<p>Real and imaginary parts of chromatic 1-D Symlet-4 wavelet</p>	<p>Chromatic and color 2-D Symlet-4 wavelet</p>
	
<p>Real and imaginary parts of chromatic 1-D Meyer wavelet</p>	<p>Chromatic and color 2-D Meyer wavelet</p>
	
<p>Real and imaginary parts of chromatic 1-D Morlet wavelet</p>	<p>Chromatic and color 2-D Morlet wavelet</p>
	
<p>Real and imaginary parts of chromatic 1-D Koif-1 wavelet</p>	<p>Chromatic and color 2-D Koif-1 wavelet</p>

	
<p>Real and imaginary parts of chromatic 1-D Koif-2 wavelet</p>	<p>Chromatic and color 2-D Koif-2 wavelet</p>
	
<p>Real and imaginary parts of chromatic 1-D Gauss-1 wavelet</p>	<p>Chromatic and color 2-D Gauss-1 wavelet</p>
	
<p>Real and imaginary parts of chromatic 1-D Gauss-2 wavelet</p>	<p>Chromatic and color 2-D Gauss-2 wavelet</p>
	
<p>Real and imaginary parts of chromatic 1-D Gauss-3 wavelet</p>	<p>Chromatic and color 2-D Gauss-3 wavelet</p>
	
<p>Real and imaginary parts of chromatic 1-D Gauss-4 wWavelet</p>	<p>Chromatic and color 2-D Gauss-4 wavelet</p>



### Ortho-unitary B-splines

Similarly to color wavelets, it is possible to construct the color splines. Let  $Spl(x)$  be a real-valued spline. We define the complex-valued (chromatic) spline as an analytic signal:

$$Spl^{Ch}(x) = Spl^{Re}(x) + jH\{Spl^{Re}(x)\} = Spl^{Re}(x) + iSpl^{Im}(x), \quad (9)$$

where  $Spl^{Im}(x) = H\{Spl^{Re}(x)\}$  is the Hilbert transform of the real-valued spline. Now we construct triplet-valued (color) wavelet basis by

$$Spl^{Col}(x) = Spl^{lu}(x) \cdot \mathbf{e}_{lu} + Spl^{Ch}(x) \cdot \mathbf{E}_{Ch} = Spl^{lu}(x) \cdot \mathbf{e}_{lu} + [Spl^{Re}(x) + jH\{Spl^{Re}(x)\}] \cdot \mathbf{E}_{Ch}. \quad (10)$$

where  $Spl^{lu}(x)$  is a real-valued wavelet basis for luminance term and  $Spl^{Ch}(x)$  is a complex-valued wavelet basis for chromatic term. We can take  $Spl^{lu}(x) \equiv Spl^{Re}(x)$ . In this case, we have

$$\begin{aligned} Spl^{Col}(x) &= Spl^{Re}(x) \cdot \mathbf{e}_{lu} + [Spl^{Re}(x) + jH\{Spl^{Re}(x)\}] \cdot \mathbf{E}_{Ch} = \\ &= Spl^{Re}(x) \cdot [\mathbf{e}_{lu} + \mathbf{E}_{Ch}] + jH\{Spl^{Re}(x)\} \cdot \mathbf{E}_{Ch}. \end{aligned} \quad (11)$$

Let  $BSpl(x)$  be, for example, a B-spline. B-splines are symmetrical, bell shaped functions constructed from a rectangular pulse:

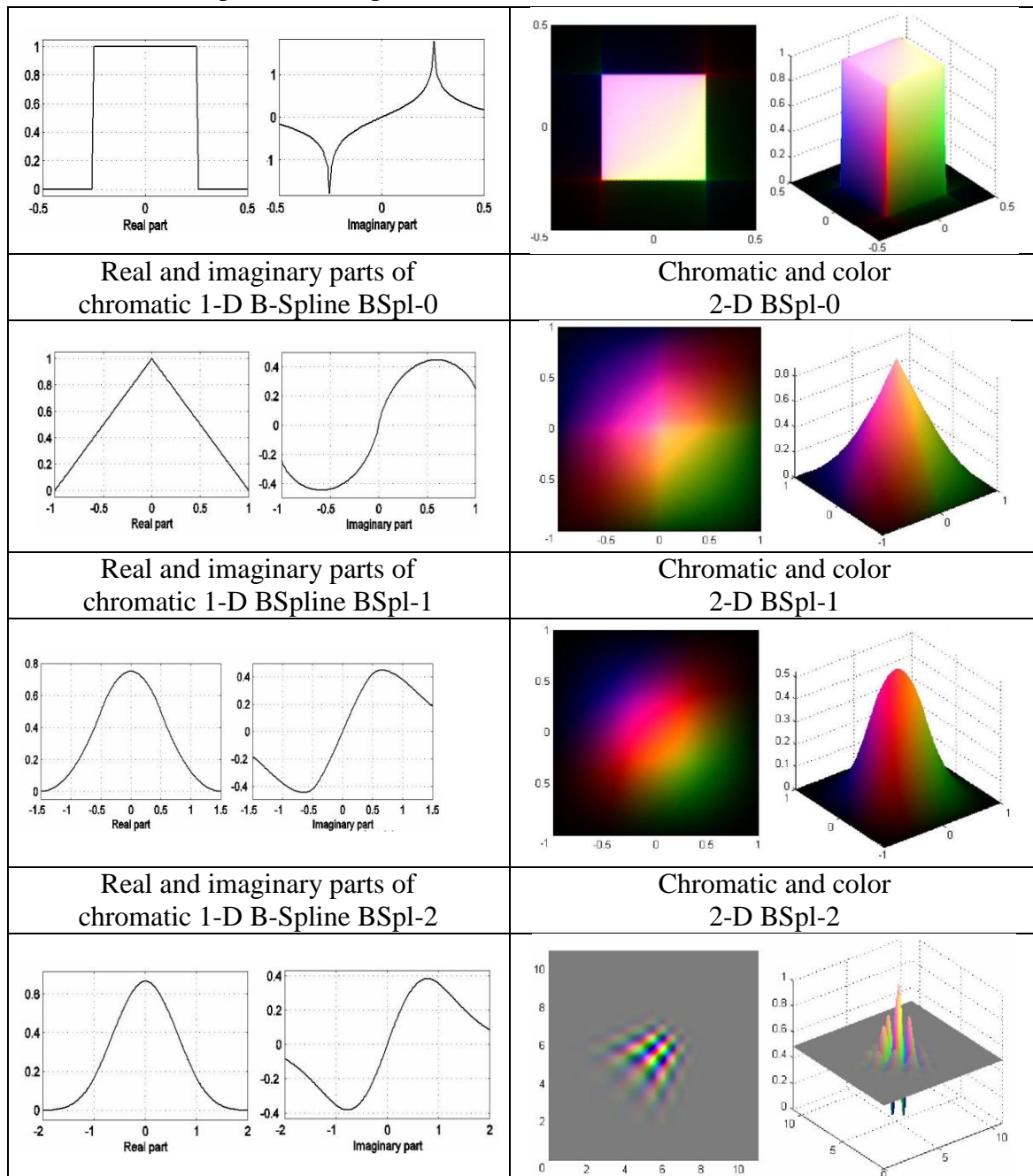


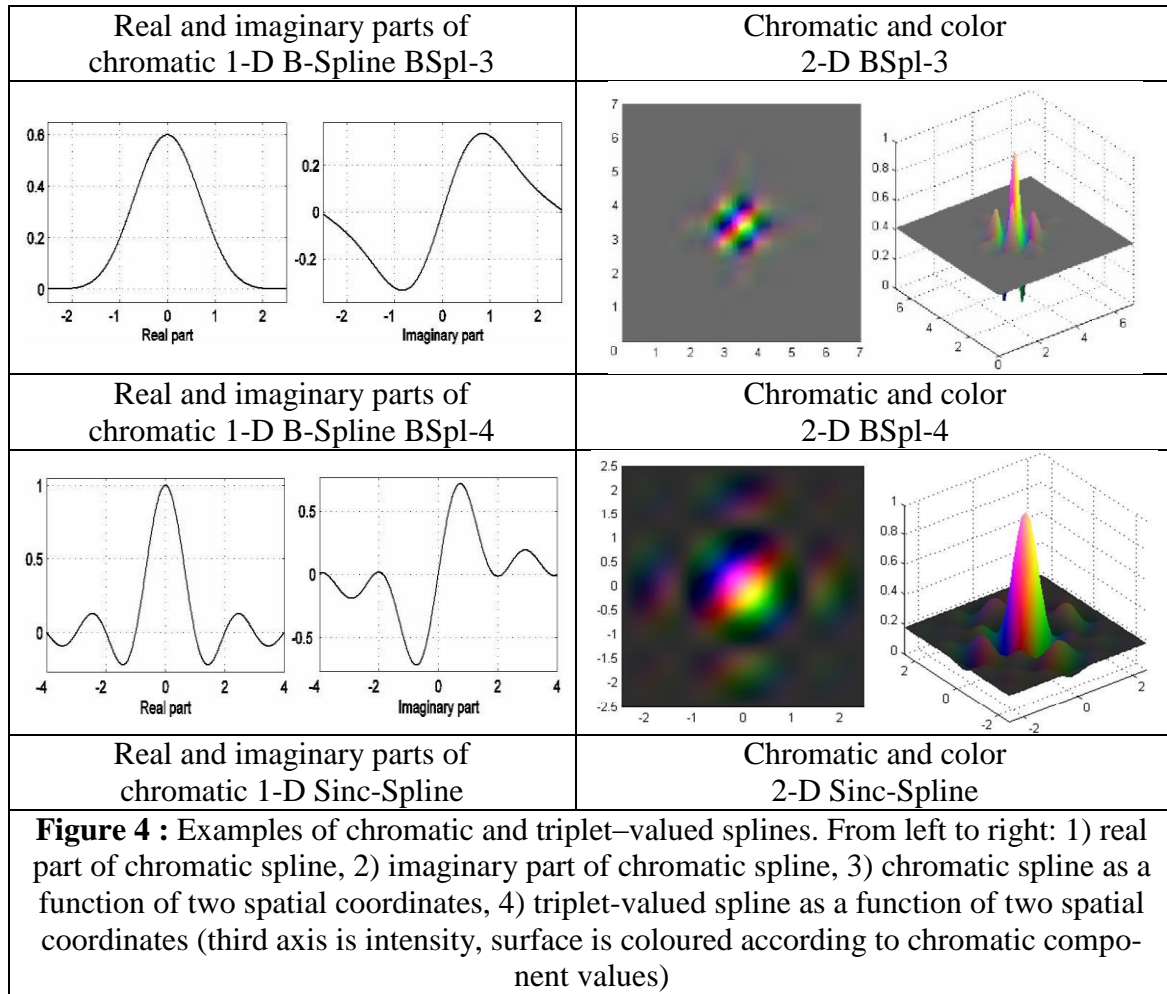
$$BSpl_0(x) = \begin{cases} 1, & -1/2 < x < 1/2, \\ 1/2, & |x| = 1/2, \\ 0, & \text{otherwise} \end{cases} \quad (12)$$

by  $BSpl_n(x) = (BSpl_{n-1} * BSpl_0)(x)$ , where  $*$  is the symbol of convolution. By this reason the color B-spline has the following form:

$$\begin{aligned} BSpl_n^{Col}(x) &= \\ &= BSpl_n^{Re}(x) \cdot \mathbf{e}_{lu} + [BSpl_n^{Re}(x) + jH\{BSpl_n^{Re}(x)\}] \cdot \mathbf{E}_{Ch} = \\ &= BSpl_n^{Re}(x) \cdot [\mathbf{e}_{lu} + \mathbf{E}_{Ch}] + jH\{BSpl_n^{Re}(x)\} \cdot \mathbf{E}_{Ch}. \end{aligned} \quad (13)$$

Examples of chromatic and triplet-valued splines are shown in Fig. 4. They are *Centaurus* of real-valued and complex-valued splines.





### Edge detection

One of the primary applications of this work could be in edge. For the edge detection, we convolve the color  $(3 \times 3)$ -masks  $\mathbf{M}_{col}(i, j)$  with color image  $\mathbf{f}_{col}(i, j)$ . We use *color Prewitt's-like* masks for detection of horizontal, vertical, and diagonal edges. As entries instead of real numbers these masks have triplet numbers:

$$\mathbf{M}_{col}^H = \begin{bmatrix} 1 & \varepsilon & \varepsilon^2 \\ 0 & 0 & 0 \\ -1 & -\varepsilon & -\varepsilon^2 \end{bmatrix}, \mathbf{M}_{col}^V = \begin{bmatrix} 1 & 0 & -1 \\ \varepsilon & 0 & -\varepsilon \\ \varepsilon^2 & 0 & -\varepsilon^2 \end{bmatrix}, \mathbf{M}_{col}^{LD} = \begin{bmatrix} \varepsilon & \varepsilon^2 & 0 \\ 1 & 0 & -\varepsilon^2 \\ 0 & -1 & -\varepsilon \end{bmatrix}, \mathbf{M}_{col}^{RD} = \begin{bmatrix} 0 & 1 & \varepsilon \\ -1 & 0 & \varepsilon^2 \\ -\varepsilon & -\varepsilon^2 & 0 \end{bmatrix}.$$

We see that triplet color detector is realized without multiplications. Fig. 5 shows result of color edge detecting

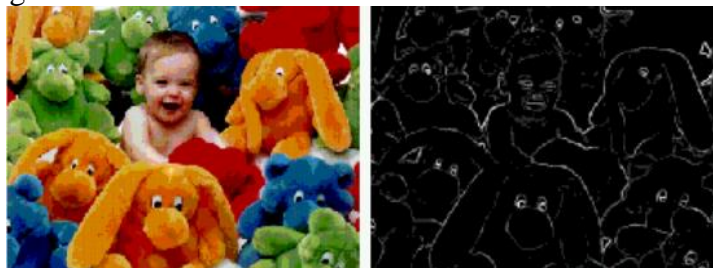


**Fig. 5:** Color edge detector. Left: original image, right: detected edges.

## Conclusion

In this study we define new methods of constructing triplet-valued (color) wavelets and splines. They are based on triplet algebra and Hilbert transform of signal. Also we presented new techniques for constructing fast Haar-like wavelet transforms and showed that effective computation requires image transforms to be considered in both RGB- and LC-formats. It is our aim to show that the use of hypercomplex algebras fits more naturally to the tasks of recognition of multicolor patterns than does the use of color vector spaces. Further work will be concentrated on application aspects of obtained results.

## Acknowledgment

This work was supported by grants the RFBR No. 17-07-00886 and by Ural State Forest Engineering's Center of Excellence in "Quantum and Classical Information Technologies for Remote Sensing Systems"

## References

- Greaves C.* On algebraic triplets // Proc. Irish Acad. 1847. Vol. 3. P. 51–54, 57–64, 80–84, 105–108.
- Labunets V., Chasovskikh V., Ostheimer E.* Algebra and geometry of multichannel images. Part 1. Hypercomplex models of retinal images // Эко-потенциал. 2016. № 4 (16).
- Labunets V., Maidan A., Rundblad-Labunets E., Astola J.* Colour triplet-valued wavelets, splines and median filters // Spectral Methods and Multirate Signal Processing, SMMSP', 2001. P. 61–70.
- Labunets V., Rundblad E., Astola J.* Is the brain a Clifford algebra quantum computer? (Chapter 25) // Applications Of Geometrical Algebras In Computer Science And Engineering, eds. L. Dorst, C. Doran & A. Lasenby, Birkhauser: Boston, 2002. P. 285–295.
- Labunets V.G., Rundblad E.V. Astola J.* Is the brain «Clifford algebra quantum computer? // Proc. of SPIE «Materials and Devices for Photonic Circuits», 2001. Vol. 4453. P. 134–145.
- Labunets-Rundblad E., Labunets V., Astola J.* Is the visual cortex a fast Clifford algebra quantum computer? // Clifford Analysis And Its Applications, eds. F. Brackx, J. Chilholm & V. Soucek, Kluwer Academic Press: Dordrecht-Boston-London. Vol. 25 of NATO Science Series. II. Mathematics, Physics and Chemistry, 2001. P. 173–182
- Labunets-Rundblad E., Labunets V., Nikitin I.* An unified approach to Fourier-Clifford–Prometheus sequences, transforms and filter banks // Computational Noncommutative Algebra and Applications, eds. J. Byrnes & G. Osteimer, Kluwer: Dordrecht and Boston and London, V. 136 of NATO Science Series, 2003a. P. 389–400.
- Labunets-Rundblad E., Maidan A., Novak P., Labunets V.* Fast color wavelet-Haar-Hartley-Prometheus transforms for image processing // Computational Noncommutative Algebra and Applications, eds. J. Byrnes & G. Osteimer, Kluwer: Dordrecht and Boston and London, volume 136 of NATO Science Series, 2003b. P. 401–412.

**Рецензент статьи:** кандидат технических наук, доцент Института экономики и управления Уральского государственного лесотехнического университета М.П. Воронов.